

## Discovery of *N*-phenyl nicotinamides as potent inhibitors of Kdr

Celia Dominguez,<sup>a,\*</sup> Leon Smith,<sup>f</sup> Qi Huang,<sup>a</sup> Chester Yuan,<sup>a</sup> Xiaohu Ouyang,<sup>h</sup> Lynn Cai,<sup>a</sup> Paul Chen,<sup>g</sup> Joseph Kim,<sup>a</sup> Timothy Harvey,<sup>a</sup> Rashid Syed,<sup>a</sup> Tae-Seong Kim,<sup>a</sup> Andrew Tasker,<sup>a,†</sup> Ling Wang,<sup>b</sup> Michael Zhang,<sup>b</sup> Angela Coxon,<sup>c</sup> James Bready,<sup>c</sup> Charles Starnes,<sup>c</sup> Danlin Chen,<sup>c</sup> Yongmei Gan,<sup>c</sup> Sessa Neervannan,<sup>e</sup> Gondi Kumar,<sup>d</sup> Anthony Polverino<sup>b</sup> and Richard Kendall<sup>b</sup>

<sup>a</sup>Chemistry Research and Discovery, One Amgen Center Drive Thousand Oaks, CA 91320, USA

<sup>b</sup>Cancer Biology, One Amgen Center Drive Thousand Oaks, CA 91320, USA

<sup>c</sup>Cancer Pharmacology, One Amgen Center Drive Thousand Oaks, CA 91320, USA

<sup>d</sup>Pharmacokinetics and Drug Metabolism, One Amgen Center Drive Thousand Oaks, CA 91320, USA

<sup>e</sup>Pharmaceutics Amgen Inc., One Amgen Center Drive Thousand Oaks, CA 91320, USA

<sup>f</sup>Bristol-Myers Squibb Pharmaceutical, Research Institute, PO Box 5400, Princeton, NJ 08543-5400, USA

<sup>g</sup>515 Oakbry Court Thousand Oaks, CA 91360, USA

<sup>h</sup>2802 Parsons Blvd #1H, Flushing, NY 11354, USA

Received 27 March 2007; revised 8 June 2007; accepted 17 July 2007

Available online 22 August 2007

**Abstract**—Inhibition of tumor-induced angiogenesis is a promising strategy in anticancer research. Neovascularization is a process required for both tumor growth and metastasis. Enhanced understanding of the underlying molecular mechanisms has led to the discovery of a variety of pharmaceutically attractive targets. Decades of investigation suggest that vascular endothelial growth factor (VEGF) and its receptors, in particular VEGFR2 or kinase insert-domain-containing receptor (Kdr), play a critical role in the growth and survival of endothelial cells in newly forming vasculature. The clinical utility of inhibitors of this receptor tyrosine kinase is currently under intense investigation. Herein we report our efforts in this arena.

© 2007 Elsevier Ltd. All rights reserved.

Angiogenesis, the development of new blood vessels, is a crucial process required for development and maintenance of various physiological and pathological conditions. Under normal circumstances angiogenesis occurs during embryonic development, wound healing, and female menstruation. Pathological angiogenesis is associated with a variety of disease states, including psoriasis, diabetic retinopathy, rheumatoid arthritis, chronic inflammation, and cancer. Tumor cells promote angiogenesis to allow proper nourishment and removal of metabolic waste.<sup>1</sup>

Vascular endothelial growth factor (VEGF) is a key pro-angiogenic cytokine that is released by almost all solid tu-

mors in response to hypoxia. The function of VEGF is mediated by two high affinity receptors expressed on vascular endothelial cells, Fms-like tyrosine kinase (Flt1 or VEGFR1) and Kdr (VEGFR2), and VEGFR3 (Flt4), found on lymphatic vessels. Messenger RNA for both Flt-1 and Kdr is up-regulated in tumor-associated endothelial cells, but not in the surrounding vasculature.<sup>2,3</sup> All are members of the receptor tyrosine kinase family, and consist of an extracellular ligand binding domain, a *trans*-membrane region, and an intracellular split kinase domain. Ligand binding effects receptor dimerization, an event that increases the intrinsic kinase activity of the non-phosphorylated protein by *trans* autophosphorylation and leads to the initiation of a classical growth factor receptor signal transduction cascade.<sup>4,5</sup> Kdr is an attractive target because of its tissue expression specificity and key role in angiogenesis. The importance of the VEGF axis in cancer therapy is highlighted by the observed clinical activity of Avastin, an antibody directed against the VEGF ligand.<sup>6</sup> The most advanced tyrosine kinase inhibi-

**Keywords:** VEGF; VEGFR-2 inhibitor; Kdr inhibitor; Angiogenesis inhibitor; Kinase inhibitor.

\* Corresponding author. Tel.: +1 310 342 5503; fax: +1 310 342 5519 (C.D.); e-mail: [celia.dominguez@chdi-inc.org](mailto:celia.dominguez@chdi-inc.org)

† Andrew Tasker has helped in the preparation of the manuscript.

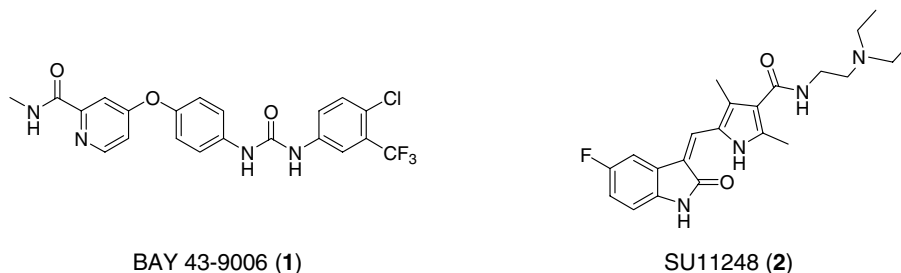


**Figure 1.** Approved Kdr inhibitors.

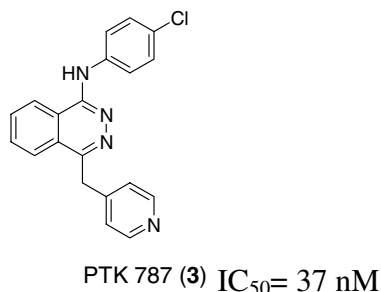


**Figure 2.** PTK 787.

tors in clinical development are BAY 43-9006 (Bayer/OSI) **1** and SU11248, (Sugen/Pfizer) **2** both of which have recently received FDA approval (Fig. 1).<sup>1</sup>

The phthalazine, PTK 787 **3**, (Fig. 2) appeared intriguing as it failed to dock into any models of Kdr derived from crystallographic data in the Protein Data Bank.<sup>7,8</sup> At first glance the aminophthalazine could be envisioned to be capable of interacting with the hinge region of the protein in a classical donor–acceptor pair fashion. This appeared, however, to be a very unlikely binding mode due to steric clash of the chlorobenzene with the C(8) proton of the phthalazine. The pyridylmethyl pendant seemed likely to be functioning as a hinge-region binding element, although it was unclear how the remainder of the molecule would be accommodated. We envisaged breaking the phthalazine N–N bond to yield an anthranilamide. This would retain most of the features of the phthalazine, be straightforward to synthesize, and moreover would be amenable to analogue work. Given the poor reactivity of an aromatic amine situated *ortho* to a carbonyl function, it seemed a pyridine-based—either 2- or 4-halo substituted—central template would provide a more attractive alternative, wherein bond construction could be effected via an aromatic nucleophilic substitution. Although useful in a synthetic sense, the introduction of this nitrogen atom represented a departure from the carbocyclic nature of the phthalazine. We therefore undertook a broad approach surveying a variety of 2-amino-substituted carboxamides derived from readily available starting materials.

The structure–activity relationships around the central template are highlighted in Table 1. Maintaining the 4-chlorophenyl amide, and the 4-(aminomethyl)pyridyl pendants as constants, the unsubstituted nicotinamide **4** proved to be potent inhibitor with a  $K_i$  of 8 nM. Further

**Table 1.** Structure–activity relationship of the central template

Compound	R	P-Kdr $n = 5$ $K_i$ ( $\mu$ M) <sup>11</sup>
<b>4</b>		0.008 <sup>a</sup>
<b>5</b>		>10 <sup>a</sup>
<b>6</b>		0.49
<b>7</b>		>10
<b>8</b>		0.14
<b>9</b>		0.12 <sup>a</sup>
<b>10</b>		0.015
<b>11</b>		>10

<sup>a</sup> UP-Kdr  $K_i$ .

substitutions exemplified by the 6-methyl **5**, or 5-bromo **6**, proved less satisfactory. Transposition of the nitrogen to yield the picolinamide **7** was very poorly tolerated. Pyrimidine **8** suffered a 10-fold loss in activity when compared to nicotinamide **4**. Thiophene **9** displayed activity comparable to the pyrimidine, and the fully carbocyclic anthranilamide **10** suffered only a twofold loss with respect to the original nicotinamide. Finally, saturation of the ring system highlighted by the cyclohexane **11**, resulted in a decrease of inhibitory activity.

The nature of the aniline substituent and the pendant aminomethylpyridine was explored via focused libraries holding the nicotinamide constant. As shown in Table 2

**Table 2.** Structure-activity relationship of nicotinamide aniline amide

Compound	R <sup>1</sup>	P-Kdr <i>n</i> = 5 <i>K</i> <sub>i</sub> (μM) <sup>11</sup>
12		0.002
13		0.004
14		0.008
15		0.009
16		0.017
17		0.019
18		0.023
19		0.010
20		0.023
21		0.091
22		0.106
23		0.177/(0.029)
24		0.259
25		0.002

**Table 2 (continued)**

Compound	R <sup>1</sup>	P-Kdr <i>n</i> = 5 <i>K</i> <sub>i</sub> (μM) <sup>11</sup>
26		0.320
27		>6.66
28		>6.66
29		>20

the aniline ring tolerated a modicum of substituents,—preferably not a large substituent *ortho* to the nitrogen linkage (compound **29**)—including alkyl chains (**17**, **22**, **26**), phenyl **18**, and carbocycles at the *para* position (**12**). The *meta*-chloro **25** showed enhanced potency with *K*<sub>i</sub> of 2 nM, respectively. Disubstitution at both *meta* and *para* positions with small groups was also well tolerated (**13**, **16**). The addition of polar functionality typified by alcohols or basic amines resulted in a decrease in activity (**27**, **28**), suggesting that interactions between this part of the molecule and the protein were hydrophobic in nature.

Variation of the aminomethylpyridine pendant provided a narrow SAR and is outlined in **Table 3**. The piperonyl

**Table 3.** Structure-activity relationship of nicotinamides varying pyridine pendant

Compound	R <sup>2</sup>	P-Kdr <i>n</i> = 5 <i>K</i> <sub>i</sub> (μM) <sup>11</sup>
19		0.01
30		0.038
31		0.07
32		0.135
33		>20

methane **30** showed good activity as did indazole **31**, although an almost order of magnitude loss compared to the starting pyridine. The *para*-fluoro benzyl analogue **32** displays modest activity ( $K_i = 135$  nM) while benzothiophene **33** is a poor inhibitor.

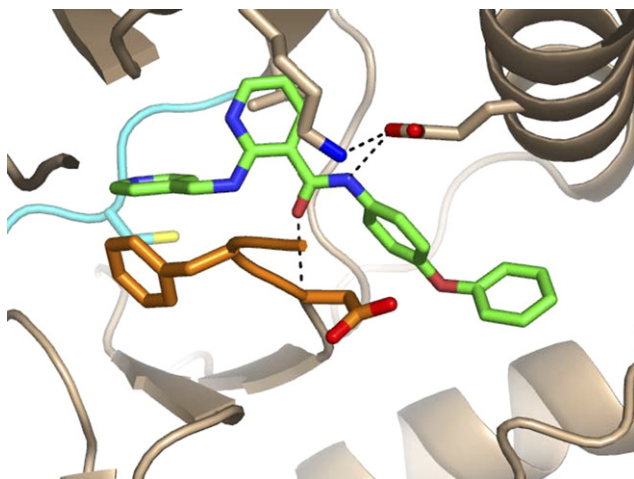


Figure 3. Compound **21** co-crystallized with Kdr (pdb 2p2i).

The paraphenoxyphenyl amide **19** proved amenable to cocrystallization with the enzyme (PDB Accession No. 2p2i). The protein adopts an Asp1046-Phe1047-Gly1048 (DFG) out conformation (Fig. 3) wherein the anilino ring reaches into an extended hydrophobic pocket resulting from the movement of this section of polypeptide chain. This conformation is not observed in the presence of ATP or the classical quinazoline-type inhibitors.<sup>8</sup> Conversely, the pendant pyridyl nitrogen forms a hydrogen bond with the hinge residue Cys919, an interaction used by both ATP and quinazolines. The conformational change in the protein exposes previously buried atoms in the ligand-binding site. The NH of the aniline amide is H-bonded with the conserved Glu885 from Helix C, and the carbonyl oxygen forms an H-bond with Asp1046 from the DFG loop. We can rationalize that the loss of activity displayed by the pyrimidine **8** was probably due to electrostatic repulsion from the oxygen of Val914, and that both C(5) and C(6) substitution create a steric clash with the backbone of the protein. The nitrogen atom of the transposed picoline **8** would result in an electrostatic repulsion with the carboxylate of Glu885.

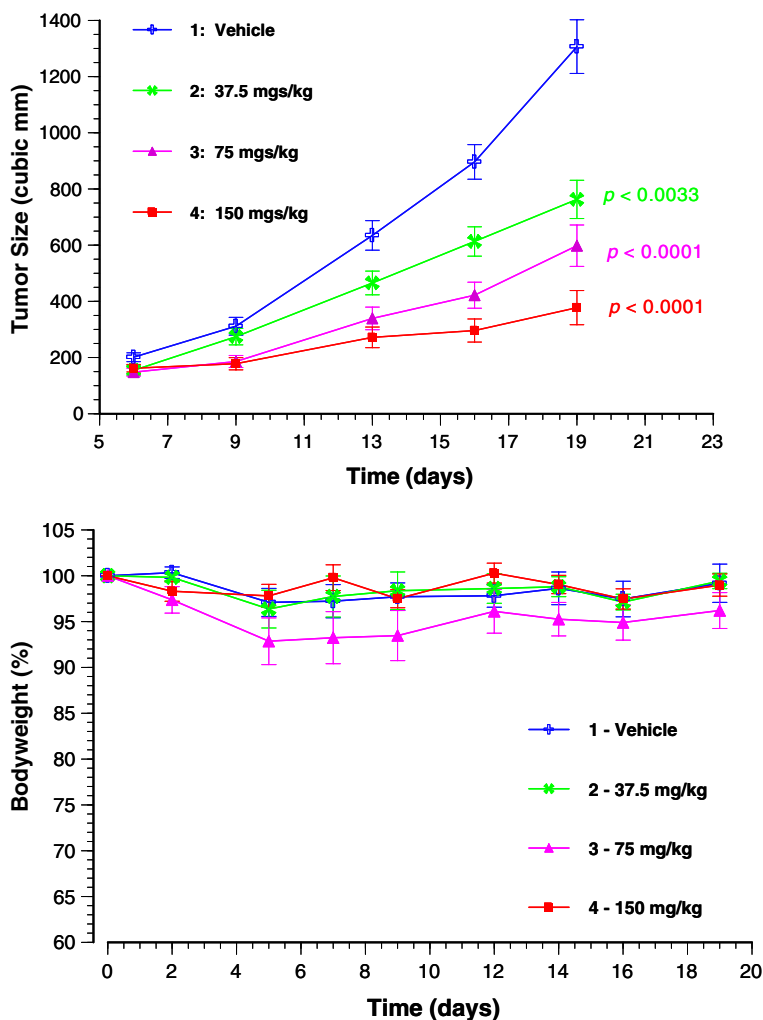


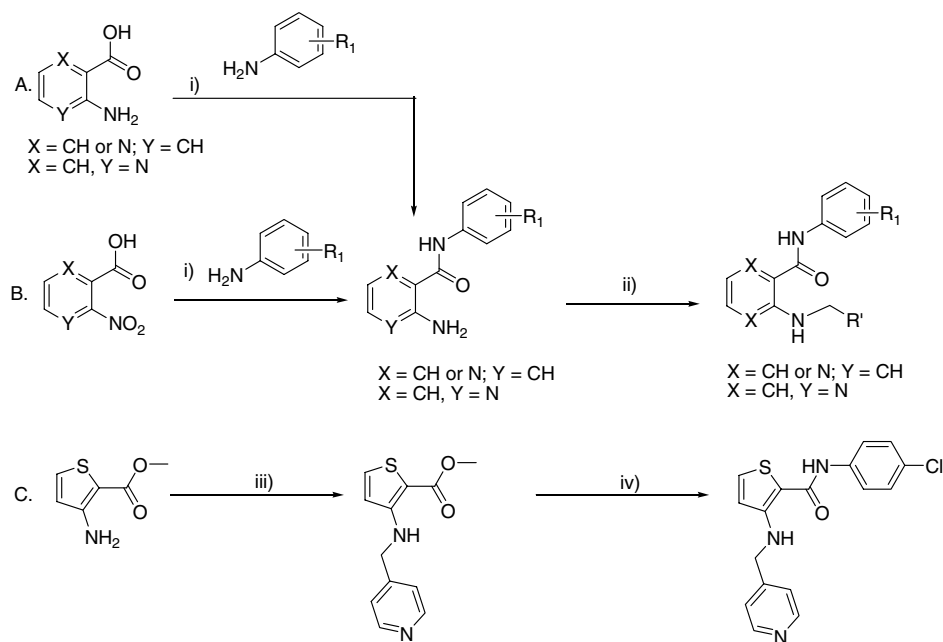
Figure 4. Compound **4** in A431 xenograft dosed po/bid.

Compounds **4** and **25** were potent in VEGF-driven HUVEC proliferation assays (8 nM and 40 nM, respectively), displayed good selectivity in bFGF-driven HUVEC proliferation with IC<sub>50</sub>s greater than 1 μM, and demonstrated good pharmacokinetics properties in the rat (compound (**4**) 100 mg/kg 45% F, Cl = 4.4 L/h/kg, AUC 20,000 ngh/mL). Accordingly, nude mice bearing an A431 human cervical epidermoid carcinoma xenograft (Fig. 4) were treated orally twice daily with compound **4**. A statistically significant delay in disease progression is realized in a dose responsive manner. This is accompanied by statistically insignificant and non-dose responsive loss of body weights.

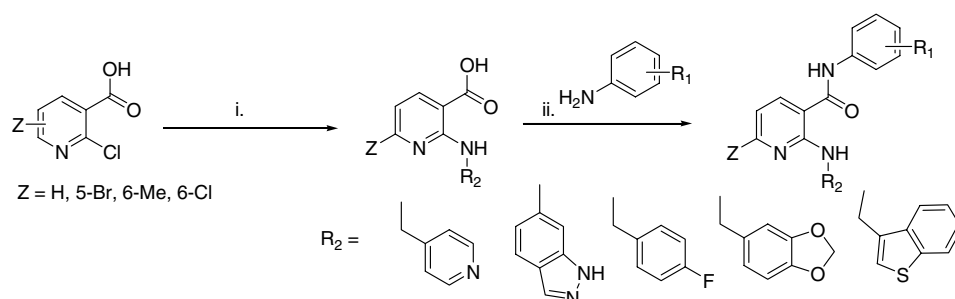
Scheme 1 illustrates the general synthesis of 2-aminonicotinamides, 3-aminopicolinamide, and the synthesis of thiophene amide **9**.<sup>9</sup> Depending on the availability of the starting material, pyridinecarboxylates bearing an activated halogen were first condensed with the appropriate aniline, then subjected to nucleophilic aromatic substitution with the pendant amine. Alternatively, 2-

nitrocarboxylates were first condensed with the appropriate aniline, then reductively aminated with an aldehyde. Thiophene **9** was prepared from methyl 3-aminothiophene-2-carboxylate via a reductive amination, ester hydrolysis, and condensation sequence. Synthesis of 2-aminonicotinamide analogues in Table 2 was carried out in a reverse fashion adopting a library format. Beginning with 2-chloronicotinic acid, displacement of the halogen with pyridylmethylamine followed by EDCI-mediated coupling with the appropriate aniline provided products in an average yield of 77% (Scheme 2).<sup>9</sup> All analogues were characterized by LCMS, <sup>1</sup>H NMR, and mass spectrometry.

In conclusion, we have identified several potent and efficacious 2-aminonicotinamide Kdr inhibitors possessing good PKDM properties. These compounds bind to the enzyme in a DFG-out conformation. Subsequent to this work, a research group at Novartis presented similar ideas.<sup>10</sup> Further work in this area will be reported in due course.



**Scheme 1.** Synthesis of 2-nicotinamides, 3-aminopicolinamide, and thiophene amide. Reagents and conditions: (i) A—1: aniline, EDC, HOBT, TEA, CH<sub>2</sub>Cl<sub>2</sub>, rt 38%, B—1: EDC, HOBT, TEA, CH<sub>2</sub>Cl<sub>2</sub>, 2: Fe, NH<sub>4</sub>Cl, EtOH/H<sub>2</sub>O, rt; (ii) R'-CHO, NaBH<sub>3</sub>CN, 15%; (iii) C—1: 4-Pyridylcarboxaldehyde, NaBH(OAc)<sub>3</sub>, DCE, 75 °C, 6 h 70%, (iv) 1—LiOH, H<sub>2</sub>O, Dioxane-MeOH·H<sub>2</sub>O (3/1/1) 150 °C 5 min, 2—EDC, HOBT, p-chloroaniline, DMF, DIPEA, 130 °C, 6 min, 15% over 2 steps.



**Scheme 2.** Synthesis of 5 and 6-substituted 2-amino nicotinamides. Reagents and condition: (i) R<sub>2</sub>NH<sub>2</sub>, sealed tube, 130 °C, 38%; (ii) EDC, DIEA, 77%.

## References and notes

1. Keren, P.; Zhu, Z. Development of angiogenesis inhibitors to vascular endothelial growth factor receptor 2: current status and future perspective. *Frontiers in Bioscience* **2005**, *10*, 1415–1439.
2. Kerbel, R. S. Tumor angiogenesis: past, present and the near future. *Carcinogenesis* **2000**, *21*, 505–515.
3. Makinen, T.; Jussila, L.; Karpanen, T.; Keitunen, M. I.; Pulkkanen, K. J.; Kauppinen, R.; Jackson, D. G.; Kubo, H.; Nishikawa, S. I.; Yla-Herttuala, S.; Alitalo, K. Inhibition of lymphangiogenesis with resulting lymphedema in transgenic mice expressing soluble VEGF receptor-3. *Nat. Med.* **2001**, *7*, 199–205.
4. Veikkola, T.; Karkkaninen, M.; Claesson-Welsh, L.; Alitalo, K. Regulation of angiogenesis via vascular endothelial growth factor receptors. *Cancer Res.* **2000**, *60*, 203–212.
5. Neufeld, G.; Cohen, T.; Gengrinovich, S.; Poltorak, Z. Vascular endothelial growth factor (VEGF) and its receptors. *FASEB J.* **1999**, *13*, 9–22.
6. Hurwitz, H.; Fehrenbacher, L.; Novotny, W.; Cartwright, T.; Hainsworth, J.; Heim, W.; Berlin, J.; Baron, A.; Griffing, S.; Holmgren, E.; Ferrara, N.; Fyfe, G.; Rogers, B.; Ross, R.; Kabbinavar, F. Bevacizumab plus irinotecan, fluorouracil, and leucovorin for metastatic colorectal cancer. *N. Engl. J. Med.* **2004**, *350*(23), 2335–2342.
7. McTigue, M. A.; Wickersham, J. A.; Pinko, C.; Showalter, R. E.; Parast, C. V.; Tempczyk-Russell, A.; Gehring, M. R.; Mroczkowski, B.; Kan, C.-C.; Villafranca, J. E.; Appelt, K. Crystal structure of the kinase domain of vascular endothelial growth factor receptor 2: a key enzyme in angiogenesis. *Structure* **1999**, *7*, 319–3308.
8. Hennequin, L. F.; Thomas, A. P.; Johnstone, C.; Stokes, E. S. E.; Ple, P. A.; Lohmann, J.-J. M.; Ogilvie, D. J.; Dukes, M.; Wedge, S. R.; Curwen, J. O.; Kendrew, J.; Lambert-van der Brempt, C. Design and structure–activity relationship of a new class of potent VEGF receptor tyrosine kinase inhibitors. *J. Med. Chem.* **1999**, *42*(26), 5369–5389.
9. Chen, G., Booker, S., Cai, G. Croghan, M., Dipeitro, L., Dominguez, C., Elbaum, D., Germain, J., Huang, Q., Kim, J., Kim, T-S., Patel, V., Smith, L., Tasker, A., Xi, N., Xu, S., Yuan, C. Preparation of Substituted Arylamines and Methods of Use as Anti-tumor Agents. WO 02/055501.
10. Manley, P.W., Bold, G. 2-Amino-Nicotinamide Derivatives and Their Use as VEGF-receptor Tyrosine Kinase Inhibitors. WO 01/55114.
11. Kinase reaction: [polyphor 96-well black round-bottomed plate; Costar 3365] Using BIO-MEK FX 60  $\mu\text{L}$  kinase reaction buffer was added to 10  $\mu\text{L}$  of P-Kdr (diluted in KRB at 42.5 nM) in all wells except those in column 12 with a final concentration of 5 nM for Kdr enzyme (Stock concentration of Kdr enzyme = 27  $\mu\text{M}$ ). This was followed by 1.6  $\mu\text{L}$  of inhibitor, which was incubated for 30 min at room temperature on a shaking platform. The reaction was started with addition of 20  $\mu\text{L}$  of 8.925  $\mu\text{M}$  ATP to the assay plates per well (final concentration of ATP 1.05  $\mu\text{M}$ ). The reaction mixture was incubated for 60 min at room temperature on a shaking platform. HTRF reaction: [Polyphor 96-well black round-bottomed plate; Costar 3365]. To Costar 3356 plate were added 80  $\mu\text{L}$  HTRF buffer, SA-APC (0.2  $\mu\text{L}/80 \mu\text{L}$ ), and EU-PT66 antibody (0.2  $\mu\text{L}/80 \mu\text{L}$ ), which was diluted with EU-PT66 70X in HTRF buffer. 5  $\mu\text{L}$  of the kinase reaction was sampled using Biomek-FX and incubated for 30 min at room temperature on a shaking platform, then read on Ruby-Star. KRB: 20 mM Tris-HCl, pH 7.5, 10 mM  $\text{MgCl}_2$ , 5 mM  $\text{MnCl}_2$ , 100 mM NaCl, 1.5 mM EGTA, 1 mM DTT, 0.2 mM SOV, and 20  $\mu\text{g}/\text{mL}$  BSA (40  $\mu\text{L}$  to 100 mL buffer/60  $\mu\text{L}$  to 150 mL buffer). HTRF buffer: 50 mM Tris-HCL, pH 7.5, 100 mM NaCl, 0.1% BSA, and 0.05% Tween 20.